A System Approach for Temperature Dependency of Impedance-Based Structural Health Monitoring

Dao Zhou[*], Jeong Ki Kim[*], Dong Sam Ha[*1], Joshua D. Quesenberry[*], and Daniel J. Inman[**]

[*]Center for Embedded Systems for Critical Applications (CESCA)
Department of Electrical and Computer Engineering
Virginia Tech, Blacksburg, VA 24061

[**]Center for Intelligent Material Systems and Structures
Virginia Polytechnic Institute and State University
310 Durham Hall Mail Code 0261
Blacksburg VA 24061

ABSTRACT

An impedance-based structural health monitoring (SHM) system employs a piezoelectric patch to excite the structure under test and capture its response. Impedance-based SHM offers several advantages over other methods such as good performance for local damage detection and simple hardware. A major problem for impedance-based SHM is temperature dependency. Specifically, baseline impedance profiles of structures vary as the ambient temperature changes. In this paper, we propose a new method to compensate the effect of temperature on baseline profiles. Our method is to select a small subset of baseline profiles for some critical temperatures and estimates the baseline profile for a given ambient temperature through interpolation. We incorporated our method into our SHM system and investigated the effectiveness of our method. Our experimental results show that (i) our method reduces the number of baseline profiles to be stored, and (ii) estimates the baseline profile of a give temperature accurately.

Keywords: structural health monitoring, SHM, impedance based method, temperature dependency, piezoelectric

1. INTRODUCTION

An impedance based structural health monitoring (SHM) system employs a piezoelectric patch to excite the structure under test and to capture its response. Impedance-based SHM offers several advantages over other methods such as good performance for local damage detection and simple hardware. A major problem for an impedance-based SHM is temperature dependency. Specifically, impedance profiles of structures vary as the ambient temperature changes. Previous studies show that the real part of the impedance is more sensitive to damage of the structure and less sensitive to the temperature compared with the imaginary part. The magnitude of peaks for the real part shrinks as the temperature increases, while the peaks (which represent its resonant frequencies) for the imaginary part shift to lower frequency band [1]. Several methods were proposed to mitigate the temperature dependency problem. Krishnamurthy et al. suggested a magnitude averaging scheme, which is to calculate the average value of the magnitude assuming a linear relationship between the magnitude and the temperature. [2]. Park et al. investigated a temperature compensation scheme in the prospective of damage metric correction. The damage metric was adjusted to eliminate the horizontal shift of impedance peaks [1].

In this paper, we present a different approach, which is to store baseline impedance profiles corresponding to the temperatures in the operating range. A straightforward method is to store impedance profiles of all temperature points in the operating temperature range, but the memory requirement is excessive. An alternative method is to store all the

[1] ha@vt.edu, phone: (540) 231-4942, fax: (540) 231-3362, www.cesca.us

Smart Sensor Phenomena, Technology, Networks, and Systems 2009, edited by Norbert G. Meyendorf, Kara J. Peters, Wolfgang Ecke, Proc. of SPIE Vol. 7293, 72930U · © 2009 SPIE · CCC code: 0277-786X/09/$18 · doi: 10.1117/12.816285

impedance profiles at a host computer and to transmit wirelessly the profile corresponding to the ambient temperature of the SHM system. However, the power consumption for the wireless transmission is a problem for an SHM system operating with a limited power resource. Our method is to select a small subset of baseline impedance profiles for some critical temperatures and estimate the baseline profile for a given ambient temperature through interpolation. To demonstrate effectiveness of our scheme, we incorporated our scheme into our impedance based SHM system.

This paper is organized as follows. Section 2 describes our impedance-based SHM system, in which the proposed method for temperature compensation is incorporated. Section 3 presents experimental results on impact of temperature to impedance profiles, and Section 4 proposes a method to compensate the temperature dependency. Section 5 concludes the paper.

2. DIGITAL SHM SYSTEM

We present our digital impedance-based SHM system [3], which is used to conduct experiments described in this paper. We describe the operation of our SHM system, impedance profiles, and damage metrics adopted for our SHM system, which are different from typical impedance-based SHM systems.

2.1 System operation and architecture

Major differences for our digital impedance-based SHM system from traditional systems lie in the excitation signal and sensing the response. Our system excites a PZT with a train of rectangular pulses instead of a sinusoidal signal and measures the phase of the response signal instead of the magnitude. Figure 1 (a) shows a pulse train, whose pulse repetition period or the fundamental frequency changes to sweep the target frequency range. Use of a pulse train simplifies the excitation signal generation and eliminates a digital-to-analog converter (DAC). A pulse train introduces harmonic terms as shown in Figure 1 (b) and (c). Harmonic terms would not cause a problem in practical sense, as they would cause the same effect for healthy and damaged structures.

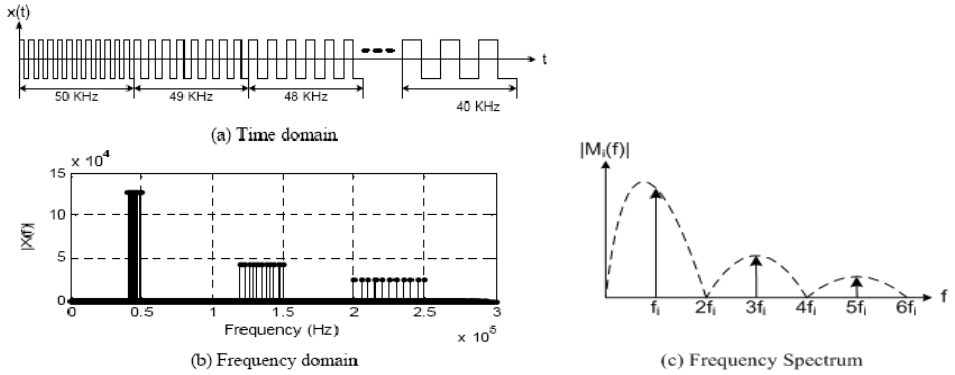

Figure1: Excitation Signal for Our Digital SHM system

The electrical admittance of a PZT patch can be expressed as $Y(jf) = G(f) + jB(f)$, where $G(f)$ and $B(f)$ are conductance and susceptance terms, respectively. It is known that the conductance term is more sensitive to damages [4]. Let $G_{base}(f)$ denote as the baseline conductance obtained from a healthy structure and $G_{SUT}(f)$ as the conductance of the structure under test (SUT). The difference between the baseline and the SUT conductance, $G_{base}(f) - G_{SUT}(f)$, indicates a damage of the structure under test. The following relationship is shown in [5].

$$G_{base}(f) - G_{SUT}(f) = k \sin[\phi_{base}(f) - \phi_{SUT}(f)] \quad (1)$$

where k is a constant, and $\phi_{base}(f)$ and $\phi_{SUT}(f)$ are the phase of $Y_{base}(f)$ and $Y_{SUT}(f)$, respectively. Expression (1) suggests that the phase difference can be used to assess a damage of a structure instead of measuring $G(f)$ directly. Our digital SHM system measures the phase difference, specifically the time difference between the voltage and the current exerted

to the structure. The measurement of the phase difference eliminates an analog-to-digital converter (ADC) and a Fast Fourier Transform (FFT) operation, which simplifies the complexity of the system in hardware and computation.

The excitation and sensing part of our SHM system is shown in Figure 2. A digital signal processing (DSP) generates a train of rectangular pulses, which are applied to a PZT patch. The opamp output voltage $V_o(t)$,which represents the current through the PZT patch, is converted into a binary signal by the comparator. The binary signal and the input voltage $V_i(t)$ are compared using an exclusive-OR (XOR) gate to measure the phase difference of the two signals, i.e., the voltage and the current of the PZT patch.

More specifically, a train of pulses with each fundamental frequency *f* is applied for 10 ms. The XOR gate continuously compares the input voltage $V_i(t)$ and the binary signal of the output voltage $V_o(t)$. The output (either 1 or 0) of the XOR gate is sampled at the rate of 100 kHz, and its value is accumulated. It can be seen easily that the resultant accumulated value is $N\phi(f)$, where N is a constant depending on the sampling rate and application of a train of pulses. The constant N is 160 for our SHM system. In order to avoid use of fractional numbers, the phase $\phi(f)$ is represented as an integer value $N\phi(f)$ for our system hereafter.

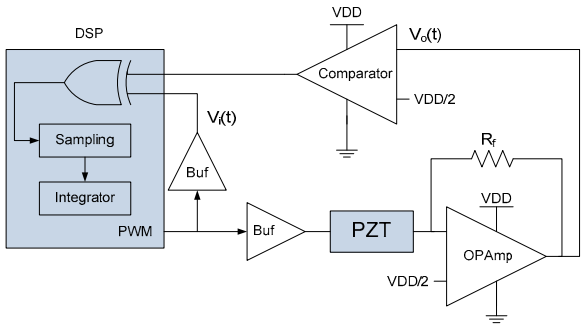

Figure 2: Excitation and Sensing Part of Our SHM System

2.2 Phase Profile and Damage Metric

The excitation frequency *f* is swept from the target frequency range from f_l to f_h with increment of 0.12 kHz. The phase profile of a structure represents a set of phase values $\phi(f_i)$'s, where f_i is discrete values between the frequency range f_l to f_h with increment of 0.12 kHz. As noted above, we use an integer value to represent a phase $\phi(f_i)$ instead of the actual phase value.

The damage metric (DM) for our system is defined as a *normalized absolute sum of difference (ASD)* between the baseline and the SUT phase profiles and is calculated as below.

$$\mathrm{DM} = \frac{\sum_{f_i=f_l}^{f_h} \left| \phi_{base}(f_i) - \phi_{SUT}(f_i) \right|}{M(f_l, f_h)} \tag{2}$$

Where $M(f_l, f_h)$ is the number of frequency points from f_l to f_h. The DM is compared against a threshold value, which may be set based on field experience. If DM is lower than the threshold value, the SUT is considered healthy. Otherwise, it is considered as damaged.

2.3 Prototyping of Our Digital SHM System

Figure 3 shows a prototype developed with a DSP (digital signal processing) evaluation board (TMS320F2812 from Texas Instruments) and a printed circuit board (PCB) for the interface circuit such as opamps. Since our system does not require an ADC and a DAC, our system is compact and power efficient.

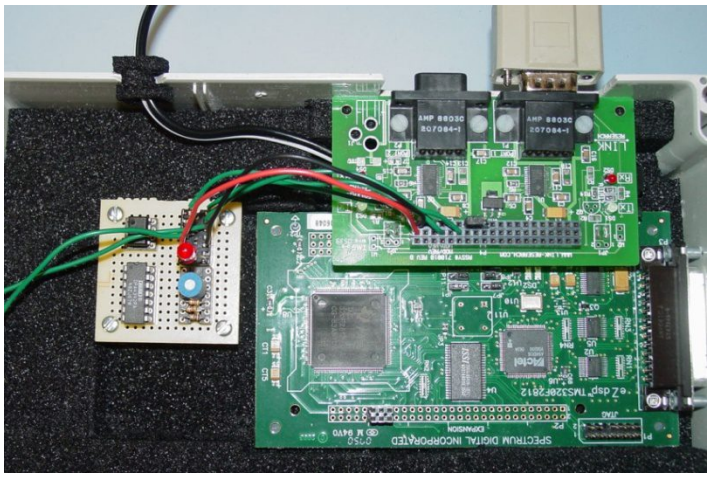

Figure 3: Prototype of Our Digital SHM System

3. EFFECT OF THE TEMPERATURE ON IMPEDANCE PROFILES

Our system measure the phase of the admittance rather than the conductance term. We tested the effect of temperature to phase profiles of the structure and show the results in this section. *We use the term impedance profile (instead of phase profile) hereafter.*

3.1 Experiment Setup

Our test structures, one healthy and one damaged, are two same size aluminum beams shown in Figure 4, and a damage was simulated with a drilled hole at the center of a beam. The test structures were hanged inside a temperature chamber (Tenney Environmental Chamber 36ST) and connected to our digital SHM system sitting outside of the chamber as shown in Figure 5. A computer is connected to the SHM system to collect and display data in real time.

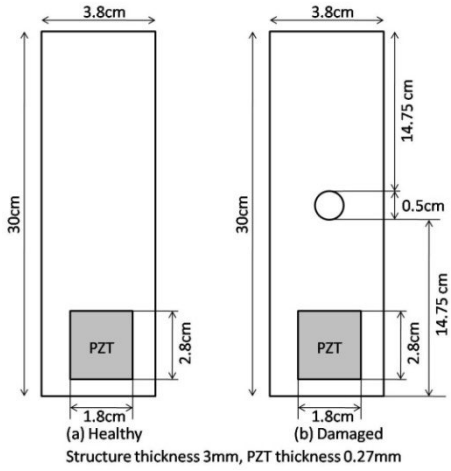

Figure 4: Test Aluminum Beams: Healthy and Damaged

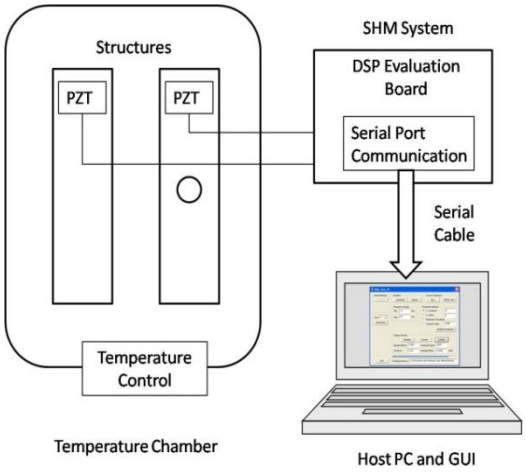

Figure 5: Experiment Setup

The temperature range for our experiments was set from -40°C to 80°C with an increment of 10°C, which results in 13 different temperatures for our experiments. The highest temperature was decided by the epoxy used to attach PZT patches, which started to lose the strength significantly beyond 80°C. We identified a frequency range from 12 kHz to 25 kHz using an impedance analyzer (HP 4294A), in which the impedance profiles of both the healthy and the damaged structures have dense resonant frequencies or peaks. We set the frequency band as the target frequency range for our

SHM system. Figure 6 shows the impedance profiles of the structures tested by the impedance analyzer at temperature 20°C.

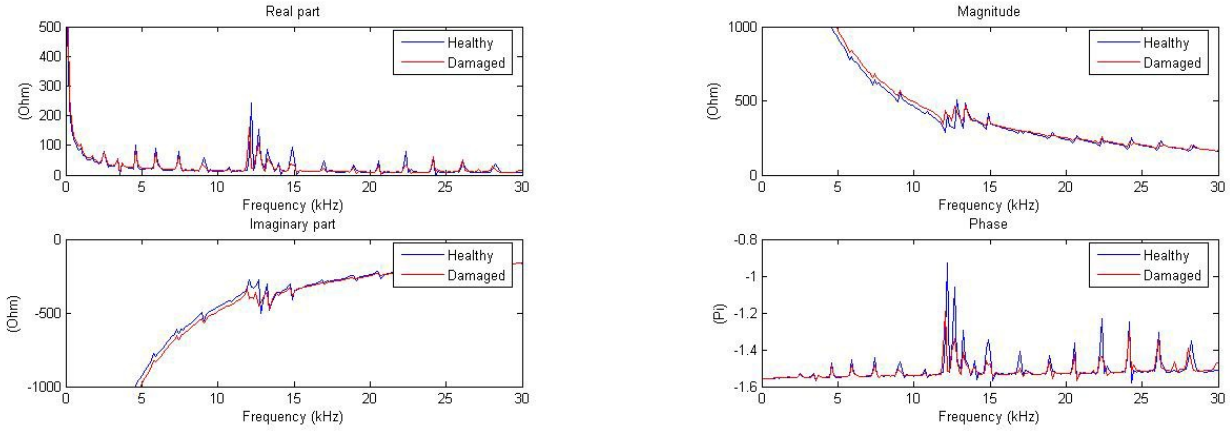

(a) Real part and Imaginary part (b) Magnitude and Phase

Figure 6: Impedance Profiles of the Healthy and the Damaged Structures

3.2 Impedance Profiles for the Temperature Range

The impedance profiles of the baseline and the damaged structures obtained by our SHM system at room temperature (20°C) are shown in Figure 7. The impedance profile of a healthy structure is noticeably different from that of a damaged one, which indicates the phase measurement adopted for our system is effective. The damage metric of the damaged structure is obtained as 62 for the damage, which is much greater than the threshold value 27.

It is interesting to note that the profiles show the target frequency range also contains many peaks. Note that the phase of the impedance is zero degree at the resonant frequency if the impedance has only one resonant frequency. Since our structures have multiple resonant frequencies at shown in Figure 6, the phase is not necessarily zero degree at a resonant frequency.

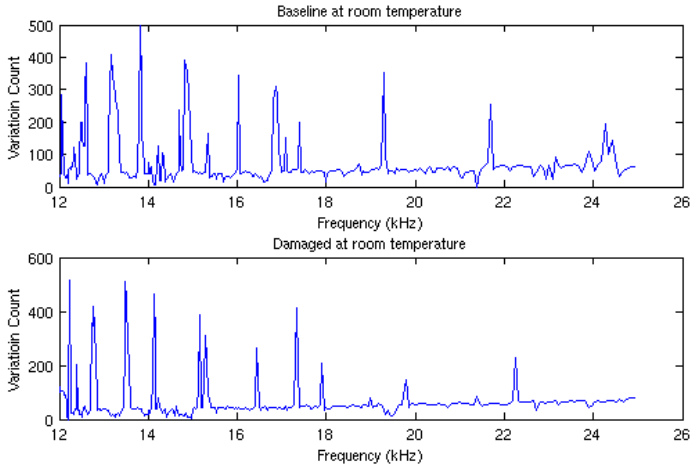

Figure 7: Impedance Profiles of the Healthy and the Damaged Structures

3.3 Temperature Effect on Impedance Profiles

We examined the effect of the temperature on impedance profiles for our test structures. We obtained baseline impedance profiles at three different temperatures, 0°C, 30°C and 60°C through three repeated experiments, at least a day apart between two consecutive experiments. Figure 8 shows baseline phase profiles for three different temperatures, and each profile is the average value of the three experiments. It is apparent that a profile shifts toward a lower frequency as the temperature increases, but the rate of the shift is not uniform. For example, the peak occurred at 13.27 KHz at temperature 0°C shifts down by 46 Hz as the temperature increases by 30°C, but by 59 Hz for the next 30°C increase. Also, most peaks shrink as temperature increases, but some peaks do not follow the trend.

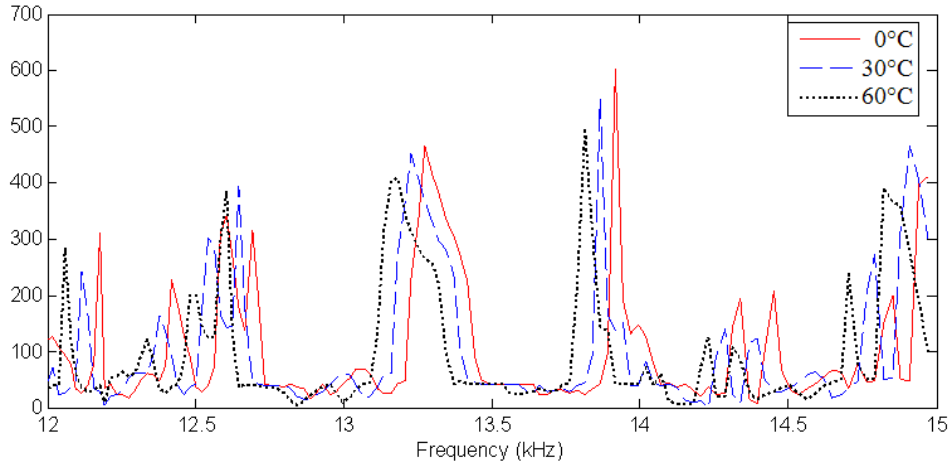

Figure 8: Temperature Effect of the Baseline Profile

3.4 Necessity for Temperature Compensation of Baseline Profiles

As expected, the impedance profiles of the damaged structure show the same tendency as baseline profiles. The two impedance profiles in Figure 9, the baseline profile at 10°C and the profile of the damaged one at 70°C, are very close. The damage metric falls below the threshold for our SHM system to fail the detection. However, the damage is detected under the baseline profile obtained at 70°C. It illustrates that use of one baseline profile without proper temperature compensation fails detection of some damages. It means that an SHM system requires sensing the ambient temperature.

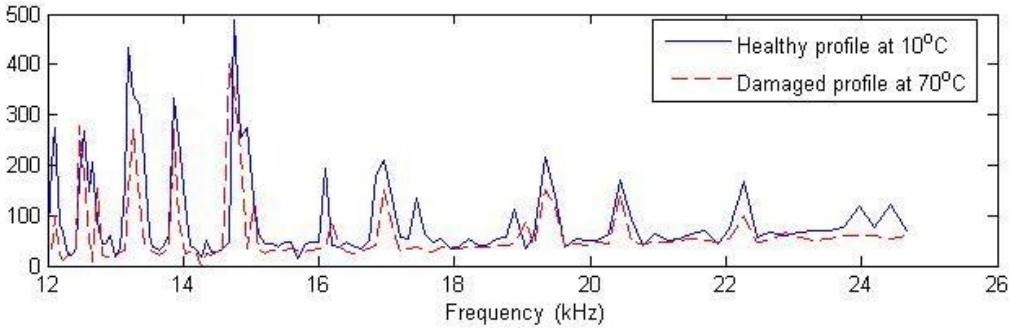

Figure 9: The Baseline Profile at 10 °C and the Profile of the Damaged Structure at 70 °C

4. COMPENSATION OF THE TEMPERATURE EFFECT

Shift of a baseline profile due to the change of the ambient temperature can cause false alarms or missed detections. A straightforward solution is to obtain and pre-store the baseline profile for each possible temperature point of the target temperature range and to use the baseline profile corresponding to the current ambient temperature. However, the

scheme requires a large memory to increase the cost of a SHM system. We present a scheme to address the problem, which is based on selection of representative baseline profiles.

4.1 Selection of Representative Baseline Profiles

Our approach is to select a small number of representative baseline profiles, from which the profile of a temperature can be estimated. A baseline profile is a nonlinear function of the temperature, which makes selection of baseline profiles at a uniform temperature interval ineffective. We propose selection of profiles based on the correlation of profiles for adjacent temperature points. The correlation coefficient ρ_{ij} of two impedance profiles $\phi_i(f)$ at temperature *i* and $\phi_j(f)$ at temperature *j* is defined as follows.

$$\rho_{ij} = \sqrt{\frac{\left[\sum_{f=f1}^{f2} \phi_i(f)\phi_j(f)\right]^2}{\sum_{f=f1}^{f2} \phi_i{}^2(f) \sum_{f=f1}^{f2} \phi_j{}^2(f)}} \tag{3}$$

A high correlation coefficient ρ_{ij} implies that the two impedance profiles at temperature *i* and temperature *j* are strongly correlated, so we can store only one of the two profiles. Further, the profile at a temperature residing between the two temperatures can be estimated with a reasonable accuracy through a linear interpolation.

Table 1 shows correlation coefficients of baseline profiles for temperatures from -40°C to 80°C with increment of 10°C. As expected, the correlation coefficient of two baseline profiles decreases as the difference between the two corresponding temperatures increases. However, the rate of the change from a pair of adjacent temperatures to the next pair is not uniform.

Table 1: Correlation Coefficients of Baseline Profiles

ρ_{ij}	-40°C	-30°C	-20°C	-10°C	0°C	10°C	20°C	30°C	40°C	50°C	60°C	70°C	80°C
-40°C	1	0.75	0.52	0.37	0.30	0.27	0.20	0.11	0.01	-0.04	-0.07	-0.05	-0.06
-30°C	0.75	1	0.75	0.49	0.39	0.25	0.19	0.18	0.09	0.02	-0.05	-0.06	-0.10
-20°C	0.52	0.75	1	0.70	0.55	0.38	0.28	0.25	0.18	0.12	0.00	-0.02	-0.08
-10°C	0.37	0.49	0.70	1	0.73	0.52	0.33	0.23	0.21	0.17	0.05	0.04	-0.05
0 °C	0.30	0.39	0.55	0.73	1	0.73	0.62	0.34	0.23	0.17	0.13	0.07	-0.02
10 °C	0.27	0.25	0.38	0.52	0.73	1	0.77	0.48	0.31	0.18	0.09	0.12	0.05
20 °C	0.20	0.19	0.28	0.33	0.62	0.77	1	0.67	0.47	0.25	0.12	0.14	0.10
30 °C	0.11	0.18	0.25	0.23	0.34	0.48	0.67	1	0.79	0.37	0.18	0.09	0.11
40 °C	0.01	0.09	0.18	0.21	0.23	0.31	0.47	0.79	1	0.63	0.30	0.17	0.11
50 °C	-0.04	0.02	0.12	0.17	0.17	0.18	0.25	0.37	0.63	1	0.52	0.34	0.22
60°C	-0.07	-0.05	0.00	0.05	0.13	0.09	0.12	0.18	0.30	0.52	1	0.65	0.43
70°C	-0.05	-0.06	-0.02	0.04	0.07	0.12	0.14	0.09	0.17	0.34	0.65	1	0.71
80°C	-0.06	-0.10	-0.08	-0.05	-0.02	0.05	0.10	0.11	0.11	0.22	0.43	0.71	1

We select representative profiles as follows. We identify a cluster of temperatures, in which *every pair* of baseline profiles within the temperature cluster has the correlation coefficient greater than or equal to 0.6. Then, we select one representative temperature from the cluster and remove all the other temperatures in the cluster from the list. In this way, we identify another cluster for the remaining temperatures and repeat the same process until all the temperature points are included.

Figure 10 shows such clusters used for our temperature selection, and the seven selected temperatures out of 13 temperatures are -40°C, -20°C, 10°C, 30°C, 50°C, 60°C and 70°C. It can be observed that low temperatures are sparsely selected, while high temperatures more densely selected. It implies that baseline profiles are more sensitive to high

temperatures. The memory saved by saving only seven baseline profiles out of 13 profiles is about 45 %.

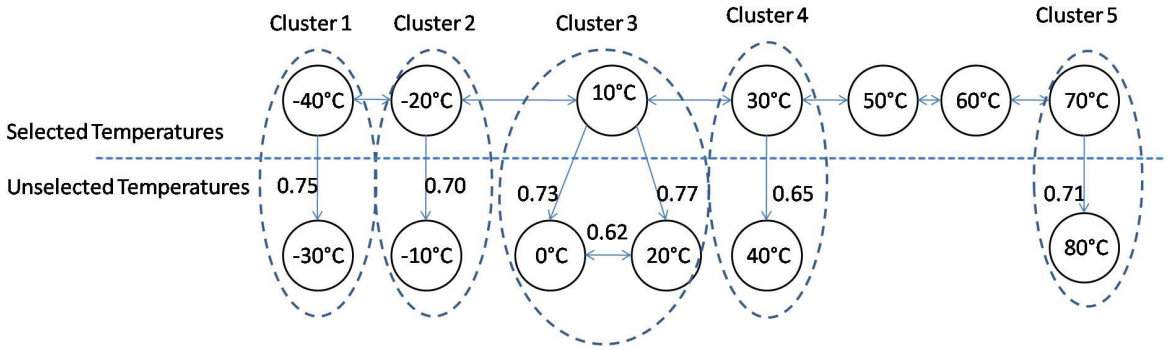

Figure 10: Cluster of Temperatures with High Correlation Coefficients

4.2 Estimation of Baseline Profiles

As observed in Section 3, a temperature change causes shift in both frequency and magnitude of a profile. We propose estimation of a profile for a given temperature using a linear interpolation between its neighboring selected temperatures. Assume the current temperature is t_x, while its neighboring selected temperatures are t_1 and t_2 such that $t_1 < t_x < t_2$. The following steps are used to estimate the profile at temperature t_x.

Step1. The profile of t_1 shifts toward a low frequency as t_1 increases toward t_2. Obtain the total amount of the frequency shift Δf from t_1 to t_2. Δf is obtained as the frequency shift maximizing the correlation between the shifted profile of t_1 and the profile of t_2.

Step2. Calculate the amount of the frequency shift from temperature t_1 and from t_2 to the target temperature t_x by dividing the total frequency shift Δf in proportion to its relative distance.

$$\Delta f_1 = \frac{t_x - t_1}{t_2 - t_1}\Delta f \ , \ \Delta f_2 = \frac{t_2 - t_x}{t_2 - t_1}\Delta f \tag{4}$$

Then, the shifted profiles $\phi_{1tox}(f)$ and $\phi_{2tox}(f)$ can be represented as follows.

$$\phi_{1tox}(f) = \phi_1(f + \Delta f_1) \ , \ \phi_{2tox}(f) = \phi_2(f - \Delta f_2) \tag{5}$$

Step 3. Calculate the profile of t_x with a linear weight on $\phi_{1tox}(f)$ and $\phi_{2tox}(f)$

$$\phi_x(f) = \frac{t_2 - t_x}{t_2 - t_1}\phi_{1tox}(f) + \frac{t_x - t_1}{t_2 - t_1}\phi_{2tox}(f) \tag{6}$$

4.3 Effectiveness of the Proposed Profile Estimation Method

We checked the effectiveness of our estimation method for two temperatures, -15°C and 35°C. The baseline profile at -15°C was constructed from the two baseline profiles of temperatures at -20°C and 10°C using the estimation method, and the constructed baseline profile is compared against a measured one at the temperature -15°C. The baseline profile at 35°C was constructed from the two baselines of temperatures at 30°C and 50°C. Figure 11 shows the two estimated profiles against their measured counterparts, and estimated and measured ones match nearly perfectly for both temperatures.

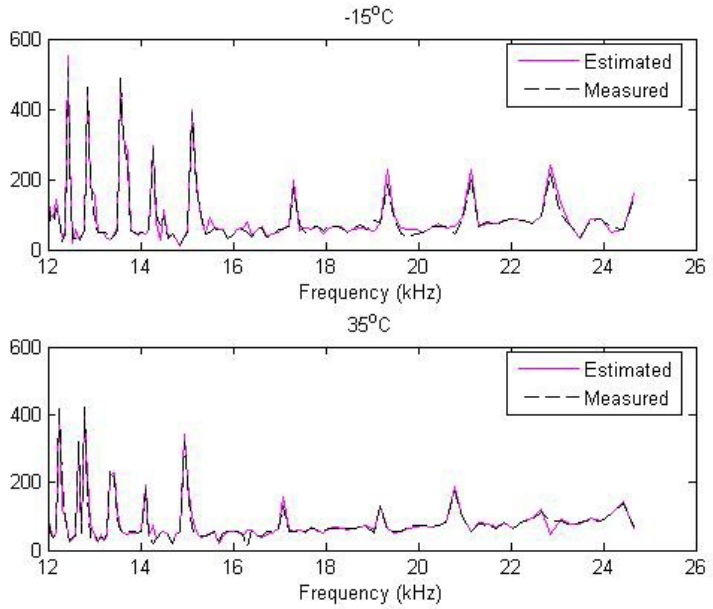

Figure 11: Estimated and Measured Baseline Profiles at Temperatures at -15°C and 35°C

In order to quantify the effectiveness, we examined the damage metrics of the profiles for the two temperatures. As noted in Section 2.2, the damage metric is obtained as the normalized absolute sum of difference between the baseline and the structure-under-test (SUT) profiles. The SUT profiles for this case are impedance profiles of the *healthy* structure at temperatures of -15 °C and 35 °C. The threshold value is set to 3σ, where σ is the variation of the baseline profiles for four repeated experiments at the room temperature of 20°C. The threshold value was obtained as 27 from the experiments.

We considered three different baseline profiles. The first baseline profile is the measured one obtained at the room temperature of 20°C. The DMs for temperatures at -15°C and 35°C are shown in the second column of Table 2. The DMs for both temperatures, 58 and 44, exceed the threshold value of 27. It means that the structure under test is considered as damaged at both temperatures due to the variations of the profiles caused by the temperature changes. The second case is the measured baseline profiles of selected neighbor temperatures. Specifically, the profile of temperature -10°C is for the temperature -15°C case and the profile of 30°C is for the temperature 35°C case. The DMs for this case are shown in the next column of the table. The DMs are decreased compared with the first case, but they are in the vicinity of the threshold value to cause possible false alarms. The final case is that the baseline profiles are those estimated through the proposed scheme. The DMs are well below the threshold value, so that no false alarm will occur. We should restate that the structure under test is the healthy one for all the three cases.

Table 2: Damage Metric for Different Baseline Profiles

Baseline	Measured Baseline at Room Temperature (20°C)	Measured Baselines at -20°C and 30°C	Estimated Baselines
-15°C	58	31	10
35°C	44	25	7

5. CONCLUSION

An impedance based SHM system employs a piezoelectric patch to excite the structure under test and capture its response. Impedance-based SHM offers several advantages over other methods such as good performance for local damage detection and simple hardware. A major problem for impedance-based SHM is temperature dependency. Specifically, baseline impedance profiles of structures vary as the ambient temperature changes. In this paper, we

proposed a new method to compensate the affect of temperature on baseline profiles. Our method is to select a small subset of baseline profiles for some critical temperatures and estimates the baseline profile for a given ambient temperature through interpolation. We incorporated our method into our digital SHM system and investigated the effectiveness of our method. Our experimental results show that (i) our method reduces the number of baseline profiles to be stored, and (ii) estimates the baseline profile of a give temperature accurately.

REFERENCES

[1] G. Park, K. Kabeya, H. H. Cudney, and D. J. Inman, "Impedance-based structural health monitoring for temperature varying applications," JSME International Journal, Series A, 42, 249-258 (1999)

[2] K. Krishnamurthy, F. Lalande, and C. A. Rogers, "Effects of temperature on the electrical impedance of piezoelectric sensors," Proc. SPIE 2717,302-310 (1996)

[3] J. Kim, B. L. Grisso, D. S. Ha, and D. J. Inman, "An all-digital low-power structural health monitoring system,", IEEE Conference on Technologies for Homeland Security,123-8 (2007)

[4] G. Park, S. Hoon, C. R. Farrar, and D. J. Inman, "Overview of piezoelectric impedance-based health monitoring and path forward," The Shock and Vibration Digest 35, 451-463 (2003)

[5] J. Kim, "Low-Power System Design for Impedance-Based Structural Health Monitoring", PhD Thesis, Virginia Polytechnic Institute and State University (2007)

[6] J. Kim, B. L. Grisso, D. S. Ha, and D. J. Inman, "Digital wideband excitation technique for impedance-based structural health monitoring systems," IEEE International Symposium on Circuits and Systems, 4 (2007).

[7] J. Kim, B. L. Grisso, D. S. Ha, and D. J. Inman, "A system-on-board approach for impedance-based structural health monitoring," Proc. SPIE 6529 PART 1 , 65290 (2007)

[8] F. Sun, C. Liang and C. A. Rogers. "Structural frequency response function acquisition via electric impedance measurement of surface bonded piezoelectric sensor/actuator" Proc. AIAA/ASME/ASCE/AHS/ASC 36th Structure, Structural Dynamics and Materials Conference, 3450-3458 (1995)

[9] G. Park, H. H. Cudney, and D. J. Inman, "Impedance-based health monitoring technique for massive structures and high-temperature structures," Proc. SPIE 3670, 461-9 (1999)

[10] D. M. Peairs, P. A. Tarazaga, and D. J. Inman, "Frequency range selection for impedance-based structural health monitoring," Transactions of the ASME. Journal of Vibration and Acoustics, vol. 129, 701-9 (2007)

[11] S. Park, Y. Chung-Bang, D. J. Inman, and P. Gyuhae, "Wireless structural health monitoring for critical members of civil infrastructures using piezoelectric active sensors," Proc. SPIE 6935, 69350-1 (2008)

[12] C. E. Woon and L. D. Mitchell, "Temperature-induced variations in structural dynamic characteristics. I. Experimental," Proc. SPIE 2868, 263-74 (1996)

[13] C. E. Woon and L. D. Mitchell, "Temperature-induced variations in structural dynamic characteristics. II. Analytical," Proc. SPIE 2868, 58-70 (1996)